STATISTICS, OPTIMIZATION AND INFORMATION COMPUTING
Stat., Optim. Inf. Comput., Vol. **x**, Month 202x, pp 0–22.
Published online in International Academic Press (www.IAPress.org)

Topp-Leone Type I Heavy-Tailed - G Power Series Class of Distributions: Properties, Risk Measures, and Applications

Wilbert Nkomo [1,2,*], Broderick Oluyede [2], Fastel Chipepa [2]

[1] *Department of Applied Statistics, Manicaland State University of Applied Sciences, Mutare, Zimbabwe.*
[2] *Department of Mathematics and Statistical Sciences, Botswana International University of Science and Technology, Botswana.*

Abstract This study presents a new class of distributions (CoDs) called the Topp-Leone type I heavy-tailed-G power series (TL-HT-GPS), along with its subclass, the Topp-Leone type I heavy-tailed log-logistic power series (TL-HT-LLOGPS) distribution. Statistical properties of this novel CoDs were derived, and actuarial risk measures were developed and numerically simulated. The maximum likelihood estimation technique was employed to estimate the unknown parameters of the model, and Monte Carlo simulations were used to evaluate the estimates' consistency. Through the use of the Topp-Leone type I heavy-tailed log-logistic Poisson (TL-HT-LLOGP) distribution, a special case of the TL-HT-LLOGPS distribution, two real data sets including a censored case, were examined to illustrate the potential of the proposed distribution. The TL-HT-LLOGP distribution was compared to a few selected non-nested competing distributions including some known heavy-tailed distributions and power series distributions. The TL-HT-LLOGP out-performed the contending distributions through various goodness-of-fit tests conducted.

Keywords Keywords:Topp-Leone, Heavy-tail, Power series distribution, Censoring, Risk measure, Estimation, Moments.

AMS 2010 subject classifications 62E30; 60E05; 62E15

DOI: 10.19139/soic-2310-5070-2039

1. Introduction

The development of new classes of probability distributions is motivated by the limitations of traditional distributions in accurately representing complex real-world data, especially in terms of kurtosis and skewness. Researchers are pushing the boundaries by incorporating extra parameters to construct more adaptable models, termed as generalized or modified distributions. Notable contributions, such as the Topp-Leone Odd Burr III-G family of distributions (FoDs) proposed by Moakofi et al. [16], the extended Topp-Leone-G FoDs by Chesneua et al. [6] and the Topp-Leone-Harris-G FoDs introduced by Oluyede et al. [19], among others, have significantly improved the ability to model extreme events and outliers in a variety of datasets.

The integration of power series distributions with continuous distributions, as exemplified in works such as the type II exponentiated half-logistic-Topp-Leone-G power series by Moakofi et al. [15] and the odd Weibull Topp-Leone-G power series by Oluyede et al. [18], the exponentiated half logistic generalized-G power series by Chipepa et al. [7], and the odd power generalized Weibull-G power series by Oluyede et al. [20], demonstrates the potential of combined distributions in accommodating diverse data patterns. These innovations highlight the versatility and efficacy of merging different distribution types to enhance modeling capabilities.

*Correspondence to: Nkomo Wilbert (Email:wilbert.nkomo@staff.msuas.ac.zw). Department of Applied Statistics, Manicaland State University of Applied Sciences, Mutare, Zimbabwe.

ISSN 2310-5070 (online) ISSN 2311-004X (print)

The Topp-Leone-G generator (TL-G) pioneered by Al-Shomrani et al. [3] excels in modeling extreme events and outliers through its adept handling of heavy-tailed behaviors and unique hazard rate function. Its application enhances the reliability of statistical analyses, especially in lifetime data contexts, underscoring the need for improved distribution models to better capture real-world complexities. As a key player among heavy-tailed distributions, the TL-G distribution accurately represents heavy tails and outliers, overcoming limitations faced by traditional distributions like Gaussian or exponential models. Its adaptability not only offers precise depictions of extreme events but also strengthens the reliability of statistical analyses, enabling researchers to derive more accurate predictions and deeper insights from their data.

The bathtub-shaped hazard rate function (hrf) of the TL-G distribution proves advantageous for lifetime data analysis, albeit constrained to the [0,1] domain. To augment the model's flexibility, numerous distributions have been generalized or amalgamated with the TL-G distribution through the addition of supplementary parameters. Nadarajah and Kotz [17] delved into the characteristics of the Topp-Leone (TL) distribution, presenting moments and a characteristic function. Ghitany et al. [9] derived various reliability measures for the TL distribution, whereas Vicaria et al. [22] introduced a two-sided generalized TL distribution. Al-Zahrani [4] scrutinized the goodness-of-fit (GoF) test for the TL distribution.

The TL-G FoDs is distinguished by its cumulative distribution function (cdf) and the matching probability density function (pdf), which are defined as follows:

$$F(x;b,\Phi) = \left[1-\bar{G}^2(x;\Phi)\right]^b \tag{1}$$

and

$$f(x;b,\Phi) = 2b\left[1-\bar{G}^2(x;\Phi)\right]^{b-1}\bar{G}(x;\Phi)g(x;\Phi), \tag{2}$$

respectively, for $b, x > 0$, where Φ is a baseline distribution parameter vector for $G(.)$ and $\bar{G}(x;\Phi) = 1 - G(x;\Phi)$.

Heavy-tailed distributions play a fundamental role in diverse domains of applied research, including reliability, actuarial science, and risk management, owing to their ability to effectively model extreme events and outliers. The type I heavy-tailed-G (HT-G) FoDs has emerged as a significant contribution to this field, stemming from the research conducted by Zhao et al. [24]. This study presents a novel FoDs that demonstrates exceptional proficiency in capturing heavy-tailed behaviors, providing invaluable insights and robust modeling capacities crucial for the comprehensive analysis and mitigation of risks across diverse domains. The cdf of the HT-G FoDs is

$$F(x;\delta,\Omega) = 1-\left(\frac{\bar{G}(x;\Omega)}{1-(1-\delta)G(x;\Omega)}\right)^{\delta} \tag{3}$$

and the pdf is

$$f(x;\delta,\Omega) \quad = \quad \frac{\delta^2 g(x;\Omega)\left[\bar{G}(x;\Omega)\right]^{\delta-1}}{\left[1-(1-\delta)G(x;\Omega)\right]^{\delta+1}}, \tag{4}$$

respectively, for $\delta, x > 0$ and Ω denotes the baseline distribution ($G(.)$) parameter vector.

Replacing the baseline cdf in Equation (1) with the HT-G distribution yields a new FoDs called Topp-Leone type I heavy-tailed-G (TL-HT-G) FoDs with cdf

$$F(x;b,\delta,\Omega) = \left(1-\left(\frac{\bar{G}(x;\Omega)}{1-(1-\delta)G(x;\Omega)}\right)^{2\delta}\right)^b \tag{5}$$

and pdf

$$f(x;b,\delta,\Omega) = 2b\delta^2\left(1-\left(\frac{\bar{G}(x;\Omega)}{1-(1-\delta)G(x;\Omega)}\right)^{2\delta}\right)^{b-1}\frac{g(x;\Omega)\left[\bar{G}(x;\Omega)\right]^{2\delta-1}}{\left[1-(1-\delta)G(x;\Omega)\right]^{2\delta+1}}, \quad (6)$$

for $b,\delta,x>0$.

This study aims to introduce a novel CoDs referred to as TL-HT-GPS. The main motivations for developing this new CoDs are:

- to develop a novel class of generalized distributions by compounding the TL-HT-G FoDs with power series distributions;
- generate distributions with different shapes, such as reversed-J, left-skewed, and right-skewed;
- to simulate various hazard rate geometries, including monotonic and non-monotonic geometries;
- to formulate heavy-tailed distributions that possess the capability of effectively representing and modeling real data sets spanning a diverse range of fields;
- to rigorously evaluate and assess the capability of the TL-HT-GPS CoDs in accurately representing risk measures, thereby enabling informed decision-making processes and the development of comprehensive risk management strategies.

The paper is structured and arranged in the following manner: Section 2 presents the development of the new CoDs, the TL-HT-GPS, including its sub-classes and special cases for specified baseline or parent distributions. Section 3 provides statistical properties of the TL-HT-GPS distribution. Parameter estimation including censoring is discussed in Section 4, while Section 5 focuses on risk measures. In Section 6, the paper presents the Monte Carlo simulation outcomes, while Section 7 showcases real data examples. Ultimately, Section 8 provides the summary.

2. The New CoDs

We introduce the Topp-Leone type I heavy-tailed-G power series (TL-HT-GPS) CoDs in this section.

Suppose we have a discrete random variable *M* that follows a power series distribution, which is presumed to be truncated at zero. The probability mass function (pmf) of *M* is defined as follows:

$$P(M=m)=\frac{a_m\theta^m}{C(\theta)}, m=1,2,3..., \quad (7)$$

where θ is a positive value, $\{a_m\}_{m\geq 1}$ is a sequence of positive real numbers and $C(\theta)=\sum_{m=1}^{\infty}a_m\theta^m$ is finite. Johnson et al. [11] presented some power series distributions and these include binomial, Poisson, geometric, and logarithmic distributions.

Consider a set of M independent and identically distributed random variables, denoted as $X_1,X_2,X_3,\ldots,X_M$, which are drawn from the TL-HT-G FoDs. Let $X_{(1)}$ represent the minimum value among $X_1,X_2,X_3,\ldots,X_M$. The expression for the conditional distribution of X given $M=m$ is given as follows:

$$F_{X_{(1)}|M=m}(x)=P\left(X_{(1)}\leq x|M=m\right)=1-\left[1-\left(1-\left[\frac{\bar{G}(x;\Omega)}{1-(1-\delta)G(x;\Omega)}\right]^{2\delta}\right)^{b}\right]^{m}.$$

The TL-HT-GPS CoDs represents the marginal distribution of $X_{(1)}$ whose cdf is expressed as follows:

$$\begin{aligned} F_{X_{(1)}}(x) &= \sum_{m=1}^{\infty} P\left(X \leq x | M=m\right) P(M=m) \\ &= \sum_{m=1}^{\infty} \left(1-\left[1-\left(1-\left[\frac{\bar{G}(x;\Omega)}{1-(1-\delta)G(x;\Omega)}\right]^{2\delta}\right)^{b}\right]^{m}\right) \frac{a_m \theta^m}{C(\theta)} \\ &= 1-\frac{C\left(\theta\left[1-\left(1-\left[\frac{\bar{G}(x;\Omega)}{1-(1-\delta)G(x;\Omega)}\right]^{2\delta}\right)^{b}\right]\right)}{C(\theta)} \end{aligned} \tag{8}$$

for $b, \delta, \theta > 0$, and the baseline cdf $G(x;\Omega)$ depends on a parameter vector Ω. The corresponding pdf is

$$f_{X_{(1)}}(x) = \frac{\theta f_{TL-HT-G}(x;b,\delta,\Omega) C'(\theta S_{TL-HT-G}(x;b,\delta,\Omega))}{C(\theta)}, \tag{9}$$

where $S_{TL-HT-G}(x;b,\delta,\Omega) = 1 - F_{TL-HT-G}(x;b,\delta,\Omega)$ is the TL-HT-G survival or reliability function, and $f_{TL-HT-G}(x;b,\delta,\Omega)$ is the corresponding pdf.

The TL-HT-GPS CoDs' pdf (from Equation (9)) is

$$\begin{aligned} f_{TL-HT-GPS}(x) &= 2b\delta^2\theta\left[1-\left(\frac{\bar{G}(x;\Omega)}{1-(1-\delta)G(x;\Omega)}\right)^{2\delta}\right]^{b-1} \frac{g(x;\Omega)\left[\bar{G}(x;\Omega)\right]^{2\delta-1}}{\left[1-(1-\delta)G(x;\Omega)\right]^{2\delta+1}} \\ &\times \frac{C'\left(\theta\left[1-\left(1-\left[\frac{\bar{G}(x;\Omega)}{1-(1-\delta)G(x;\Omega)}\right]^{2\delta}\right)^{b}\right]\right)}{C(\theta)}. \end{aligned} \tag{10}$$

If we modify the baseline cdf $G(x;\Omega)$ and specify the power series distribution, various sub-classes, and special cases of the TL-HT-GPS CoDs can be derived. The hrf and reverse hazard functions (rhrf) of the TL-HT-GPS CoDs are respectively given by

$$\begin{aligned} h_{TL-HT-GPS}(x) &= 2b\delta^2\theta\left[1-\left(\frac{\bar{G}(x;\Omega)}{1-(1-\delta)G(x;\Omega)}\right)^{2\delta}\right]^{b-1} \frac{g(x;\Omega)\left[\bar{G}(x;\Omega)\right]^{2\delta-1}}{\left[1-(1-\delta)G(x;\Omega)\right]^{2\delta+1}} \\ &\times \frac{C'\left(\theta\left[1-\left(1-\left[\frac{\bar{G}(x;\Omega)}{1-(1-\delta)G(x;\Omega)}\right]^{2\delta}\right)^{b}\right]\right)}{C\left(\theta\left[1-\left(1-\left[\frac{\bar{G}(x;\Omega)}{1-(1-\delta)G(x;\Omega)}\right]^{2\delta}\right)^{b}\right]\right)}, \end{aligned} \tag{11}$$

and

$$\tau_{TL-HT-GPS}(x) = \frac{2b\delta^2\theta\left[1-\left(\frac{\bar{G}(x;\Omega)}{1-(1-\delta)G(x;\Omega)}\right)^{2\delta}\right]^{b-1} C'\left(\theta\left[1-\left(1-\left[\frac{\bar{G}(x;\Omega)}{1-(1-\delta)G(x;\Omega)}\right]^{2\delta}\right)^{b}\right]\right)}{C(\theta) - C\left(\theta\left[1-\left(1-\left[\frac{\bar{G}(x;\Omega)}{1-(1-\delta)G(x;\Omega)}\right]^{2\delta}\right)^{b}\right]\right)}. \tag{12}$$

2.1. Special Cases

Considering the log-logistic to be the parent distribution with cdf $G(x;\beta) = 1-(1+x^{\beta})^{-1}$ and $g(x;\beta) = \beta x^{\beta-1}(1+x^{\beta})^{-2}$, for $\beta, x > 0$, and letting $1+x^{\beta} = \eta$, we have the Topp-Leone type I heavy-tail log-logistic-G power series (TL-HT-LLOGPS) CoDs with cdf

$$F_{TL-HT-LLOGPS}(x) = 1 - \frac{C\left(\theta\left(1-\left(1-\left[\frac{\eta^{-1}}{1-(1-\delta)(1-\eta^{-1})}\right]^{2\delta}\right)^{b}\right)\right)}{C(\theta)}, \tag{13}$$

and pdf

$$\begin{aligned} f_{TL-HT-LLOGPS}(x) &= 2b\theta\delta^{2}\left[1-\left(\frac{\eta^{-1}}{1-(1-\delta)(1-\eta^{-1})}\right)^{2\delta}\right]^{b-1}\frac{\beta x^{\beta-1}\eta^{-2}\left[\eta^{-1}\right]^{2\delta-1}}{\left[1-(1-\delta)(1-\eta^{-1})\right]^{2\delta+1}} \\ &\times \frac{C'\left(\theta\left(1-\left(1-\left[\frac{\eta^{-1}}{1-(1-\delta)(1-\eta^{-1})}\right]^{2\delta}\right)^{b}\right)\right)}{C(\theta)} \end{aligned} \tag{14}$$

for $b, \theta, \delta, \beta > 0$.

The Topp-Leone type I heavy-tail log-logistic Poisson (TL-HT-LLOGP), Topp-Leone type I heavy-tail log-logistic geometric (TL-HT-LLOGG) and the Topp-Leone type I heavy-tail log-logistic logarithmic (TL-HT-LLOGL) distributions are the sub-models of the TL-HT-GPS CoDs to be considered.

(a) TL-HT-LLOGP Distribution
The TL-HT-LLOGP cdf is

$$F_{TL-HT-LLOGP}(x) = 1 - \frac{\exp\left(\theta\left(1-\left(1-\left[\frac{1}{\eta(1-(1-\delta)(1-\eta^{-1}))}\right]^{2\delta}\right)^{b}\right)\right)-1}{\exp(\theta)-1},$$

the pdf is

$$\begin{aligned} f_{TL-HT-LLOGP}(x) &= 2b\delta^{2}\theta\left[1-\left(\frac{1}{\eta(1-(1-\delta)(1-\eta^{-1}))}\right)^{2\delta}\right]^{b-1}\frac{\beta x^{\beta-1}\eta^{-2}\left[(1+x^{\beta})^{-1}\right]^{2\delta-1}}{\left[1-(1-\delta)(1-\eta^{-1})\right]^{2\delta+1}} \\ &\times \frac{\exp\left(\theta\left(1-\left(1-\left[\frac{\eta^{-1}}{1-(1-\delta)(1-\eta^{-1})}\right]^{2\delta}\right)^{b}\right)\right)}{\exp(\theta)-1} \end{aligned}$$

for $b, \theta, \delta, \beta, x > 0$.

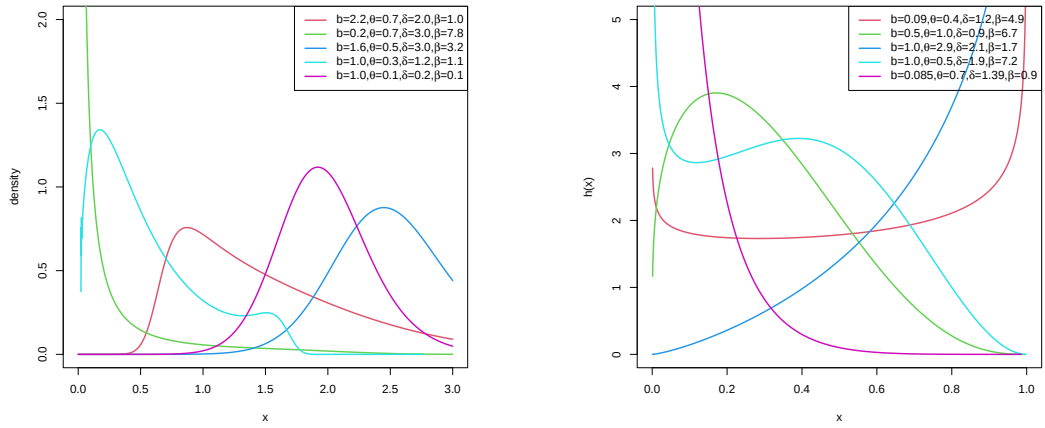

(a) (b)

Figure 1. Graphical representations of the TL-HT-LLOGP distribution, showcasing the pdf and hrf plots.

Figure [1] illustrates the versatile nature of the TL-HT-LLOGP distribution, which can exhibit virtual symmetry, positive skewness, negative skewness, or a reversed-J shape. The hrf exhibits a diverse range of shapes including bathtub, inverted bathtub, bathtub followed by inverted bathtub, increasing and decreasing shapes.

(b) TL-HT-LLOGG Distribution
The TL-HT-LLOGG cdf is

$$F_{TL-HT-LLOGG}(x) = 1 - \frac{(1-\theta)\left(1-\left(1-\left[\frac{\eta^{-1}}{1-(1-\delta)(1-\eta^{-1})}\right]^{2\delta}\right)^{b}\right)}{1-\theta\left(1-\left(1-\left[\frac{\eta^{-1}}{1-(1-\delta)(1-\eta^{-1})}\right]^{2\delta}\right)^{b}\right)},$$

the pdf is

$$\begin{aligned} f_{TL-HT-LLOGG}(x) &= 2b\theta\delta^2\left[1-\left(\frac{1}{\eta(1-(1-\delta)(1-\eta^{-1}))}\right)^{2\delta}\right]^{b-1}\frac{\beta\,(1-\theta)\,x^{\beta-1}\eta^{-2}\left[\eta^{-1}\right]^{2\delta-1}}{\left[1-(1-\delta)(1-\eta^{-1})\right]^{2\delta+1}} \\ &\times \left[1-\theta\left(1-\left(1-\left[\frac{1}{\eta(1-(1-\delta)(1-\eta^{-1}))}\right]^{2\delta}\right)^{b}\right)^{-2}\right] \end{aligned}$$

for $b, \theta, \delta, \beta > 0$ and $x > 0$.

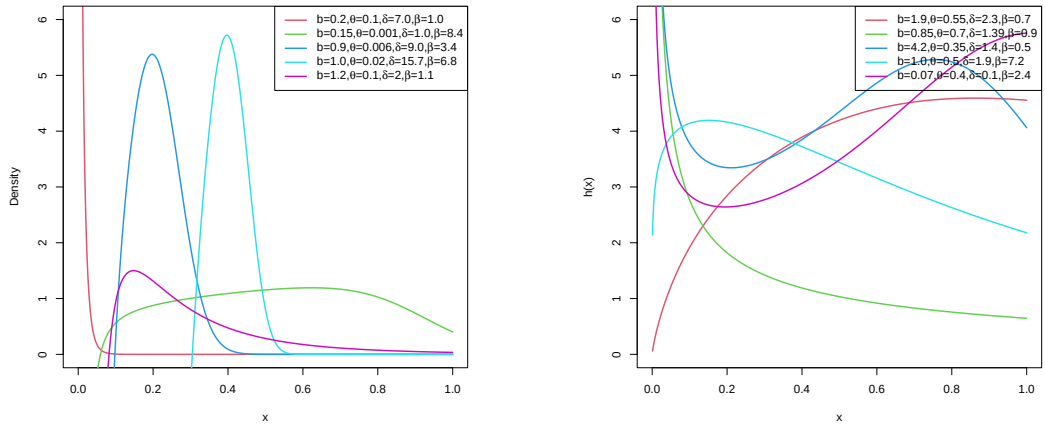

(a) (b)

Figure 2. Density and hrf plots for the TL-HT-LLOGG distribution

Figure [2] demonstrates the potential positive skewness or reversed-J shape of the TL-HT-LLOGG distribution. Additionally, the hrf displays decreasing, increasing, bathtub, inverted bathtub as well as bathtub followed by inverted bathtub shapes.

(c) TL-HT-LLOGL Distribution
The TL-HT-LLOGL cdf is

$$F_{TL-HT-LLOGL}(x) = 1 - \log\left(1 - \theta\left(1 - \left(1 - \left[\frac{\eta^{-1}}{1-(1-\delta)(1-\eta^{-1})}\right]^{2\delta}\right)^{b}\right)\right),$$

the pdf is

$$f_{TL-HT-LLOGL}(x) = 2b\theta\delta^2\left[1 - \left(\frac{1}{\eta(1-(1-\delta)(1-\eta^{-1}))}\right)^{2\delta}\right]^{b-1}\frac{\beta x^{\beta-1}\eta^{-2/delta-1}}{[1-(1-\delta)(1-\eta^{-1})]^{2\delta+1}} \times \frac{\left(1-\theta\left[1-\left(1-\left[\frac{1}{\eta(1-(1-\delta)(1-\eta^{-1}))}\right]^{2\delta}\right)^{b}\right]\right)}{-\log(1-\theta)}$$

for $b, \delta, \beta > 0, x > 0$ and $0 < \theta < 1$.

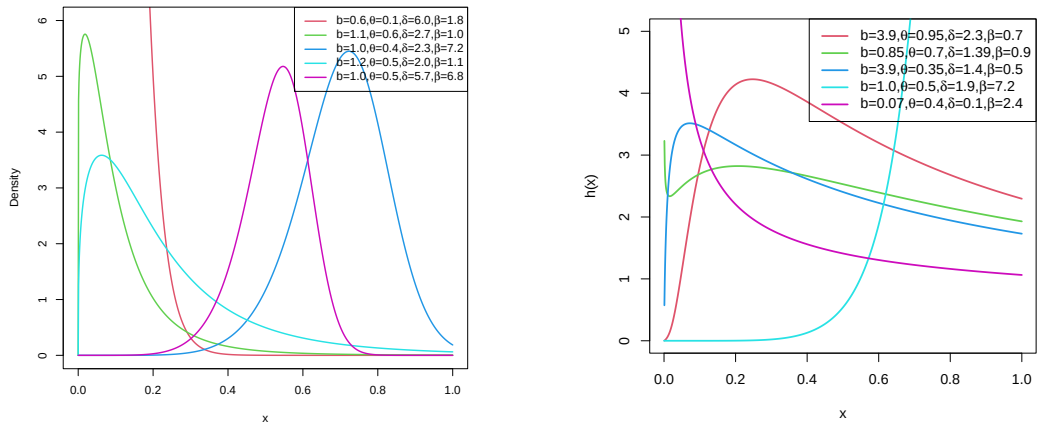

(a) (b)

Figure 3. Visualizations of the pdf and hrf for the TL-HT-LLOGL distribution

Figure [3] presents important insights into the TL-HT-LLOGL distribution. It highlights the distribution's versatility, showing that it can take on various shapes, ranging from almost symmetric to positively skewed, negatively skewed, or reversed-J. The hrf demonstrates distinct patterns, including increasing and decreasing trends, inverted bathtub, and bathtub followed by inverted bathtub shapes.

3. Quantile Function, Linear Representation, Moments and Incomplete Moments

This section contains various statistical properties associated with the TL-HT-GPS CoDs. These include the quantile function, the q^{th} moment, incomplete moments, order statistics, Rényi entropy, and probability weighted moments.

3.1. Quantile Function

The quantile function is utilized for calculating percentiles, detecting outliers, and establishing confidence intervals. It also plays a crucial role in risk assessment, finance, and decision-making processes. The TL-HT-GPS distribution's quantile function, $(Q_X(q))$ is

$$Q_X(q) = G^{-1}\left[\frac{\left(1-\left[\frac{\theta-[C^{-1}C(\theta)(1-q)]}{\theta}\right]^{\frac{1}{b}}\right)^{\frac{1}{2\delta}}}{1+(1-\delta)\left(1-\left[\frac{\theta-[C^{-1}C(\theta)(1-q)]}{\theta}\right]^{\frac{1}{b}}\right)^{\frac{1}{2\delta}}}\right] \tag{15}$$

for $0 \leq q \leq 1$. The quantile values of the TL-HT-GPS CoDs can be computed using numerical techniques in R, given the baseline cdf $G(\cdot)$ and the function $C(\theta)$. For detailed derivations, please refer to the **web appendix** section.

3.2. Linear Representation

This subsection gives a density expansion of the TL-HT-GPS CoDs. Properties of the TL-HT-GPS CoDs are derived from this expansion. The TL-HT-GPS distribution pdf can be written as

$$f(x) = \sum_{r=0}^{\infty} \eta_{r+1} g_{r+1}(x;\Omega), \tag{16}$$

where $g_{r+1}(x;\Omega) = (r+1)g(x;\Omega)G^r(x;\Omega)$ represents the exponentiated-G (Expo-G) distribution with power parameter $(r+1)$, and

$$\begin{aligned}\eta_{r+1} &= \sum_{l,n,p,q=0}^{\infty}\sum_{m=1}^{\infty}(-1)^{l+n+q+r}2b\delta^2(1-\delta)^p\binom{m-1}{l}\binom{b(l+1)-1}{n}\\ &\times \binom{2\delta(n+1)+p}{p}\binom{p}{q}\binom{q+2\delta-1}{r}\frac{ma_m\theta^m}{C(\theta)}\left(\frac{1}{r+1}\right),\end{aligned} \tag{17}$$

is the linear component. The TL-HT-GPS CoDs can be represented as an infinite linear combination of exponentiated-G (Expo-G) densities. This formulation allows for the direct derivation of various statistical properties including order statistics, entropy, and probability weighted moments can be directly derived. For comprehensive insights into this expansion and additional statistical properties, please consult the **web appendix** for detailed derivations.

3.3. Moments and Incomplete Moments

In statistics, moments serve as indicators of the distribution's form and spread, detailing both the central tendency and variability within a dataset. Incomplete moments are fundamental components essential for measuring inequality; metrics like the Lorenz curve and Gini coefficients rely on these incomplete moments, illustrating their importance in assessing wealth inequalities (McDonald and Butler [14]).

If Y_{r+1} is an Expo-G distributed random variable with power parameter $(r+1)$, then, the q^{th} moment of the TL-HT-GPS CoDs is

$$E(X^q) = \sum_{r=0}^{\infty} \eta_{r+1} E(Y_{r+1}^q),$$

where η_{r+1} is specified by Equation (17) and $E(Y_{r+1}^q)$ is the q^{th} moment of Y_{r+1}. The q^{th} incomplete moment is

$$I_X(t) = \int_0^t x^q f(x)dx = \sum_{r=0}^{\infty} \eta_{r+1} I_{r+1}(t;q,\Omega),$$

where $I_{r+1}(t;q,\Omega) = \int_0^t x^q g_{r+1}(x;\Omega)dx$ denotes the incomplete moment of Y_{r+1}. We state the moment generating function (mgf) of X as

$$M_X(t) = \sum_{r=0}^{\infty} \eta_{r+1} E(e^{tY_{r+1}}),$$

where $E(e^{tY_{r+1}})$ is the mgf of Y_{r+1} and η_{r+1} is defined in Equation (17). The computation of statistical measures such as the coefficient of skewness (CS), coefficient of variation (CV), coefficient of kurtosis (CK), variance (σ^2), and standard deviation (σ) becomes straightforward once the necessary information is available. Bonferroni and Lorenz curves for the TL-HT-GPS can also be obtained from incomplete moments of the distribution.

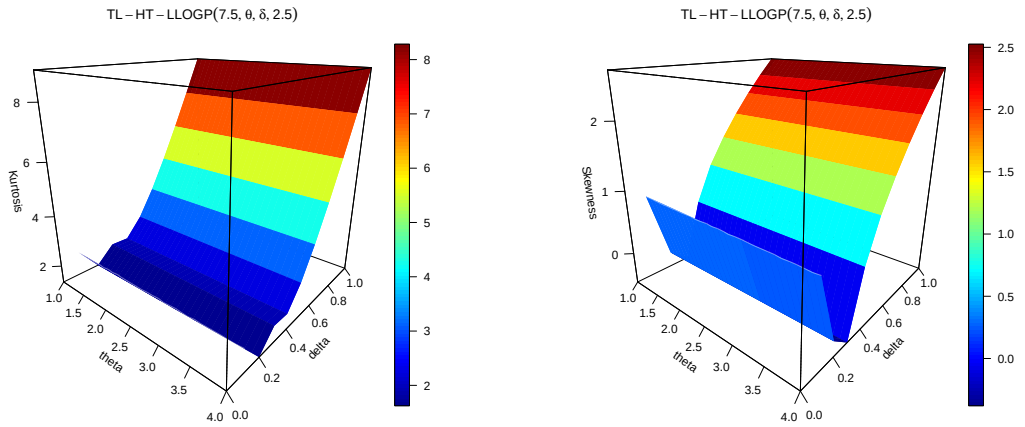

(a) (b)

Figure 4. Some 3D plots of the TL-HT-LLOGP distribution's skewness and kurtosis

Figure [4] illustrates that the TL-HT-LLOGP distribution is capable of representing data with varying degrees of kurtosis and skewness after fixing b and β.

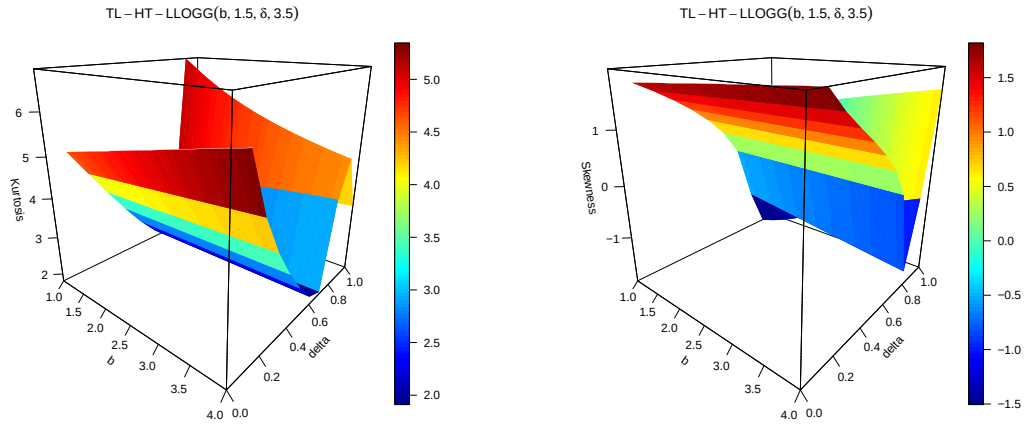

(a) (b)

Figure 5. 3D plots of the TL-HT-LLoGG distribution's skewness and kurtosis

Figure [5] demonstrates varying levels of kurtosis and skewness for the TL-HT-LLoGG distribution after fixing θ and β.

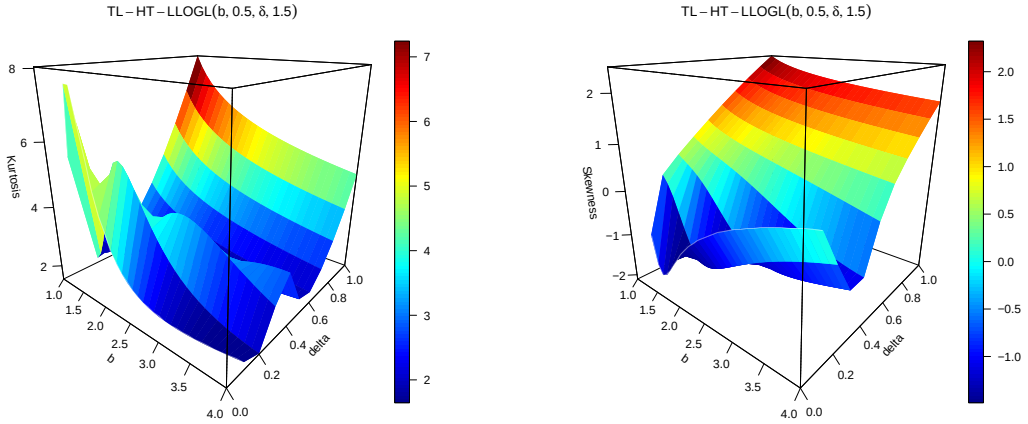

(a) (b)

Figure 6. 3D plots of the TL-HT-LLOGL distribution's skewness and kurtosis

After controlling for θ and β, Figure [6] demonstrates that the TL-HT-LLOGL distribution displays different degrees of kurtosis and skewness as b and δ increase.

4. Estimation

In this section, our primary objective is to estimate the unknown parameters of the TL-HT-GPS CoDs. We aim to achieve this by utilizing the maximum likelihood estimation (MLE) technique. The optimization process for estimating distribution parameters followed an iterative approach, starting with an initial set of parameter estimates informed by domain knowledge and preliminary data analysis. To make the process more robust, multiple random initializations were tried, and the one that led to the best objective function value (the negative log-likelihood) was selected. The parameter estimates were then updated in each iteration using the maximum likelihood estimation algorithm, and after each update, the convergence of the optimization was checked by monitoring the stabilization of the negative log-likelihood. The iterations continued until the objective function reached a stable value, indicating that the parameters had converged to an optimal solution. This combination of iterative refinement, informed initialization, and convergence checking ensures that the final parameter estimates are reliable and accurate, providing a trustworthy model of the underlying distribution and making the optimization process less sensitive to the choice of initial parameter estimates.

4.1. Estimation in the Absence of Censoring

The aim of this subsection is to obtain the MLEs for the parameters linked to the TL-HT-GPS CoDs.

Consider a random sample of size n denoted by $X_i \sim$ TL-HT-GPS, and let $\Delta = (b, \delta, \theta, \Omega)^T$ represent the

parameter vector. The log likelihood function $\ell = \ell(\Delta)$ can be expressed as

$$\begin{aligned}\ell = \ell(\Delta) &= 2n\log(\delta) + n\log(2b\theta) + \sum_{i=1}^{n}\log[g(x_i;\Omega)] + (b-1)\sum_{i=1}^{n}\log\left[1-\left(\frac{\bar{G}(x_i;\Omega)}{1-(1-\delta)G(x_i;\Omega)}\right)^{2\delta}\right] \\ &+ (2\delta-1)\sum_{i=1}^{n}\log[\bar{G}(x_i;\Omega)] - (2\delta+1)\sum_{i=1}^{n}\log\left[1-(1-\delta)G(x_i;\Omega)\right] - \sum_{i=1}^{n}\log\left[C(\theta)\right] \\ &+ \sum_{i=1}^{n}\log\left\{C'\left(\theta\left[1-\left(1-\left[\frac{\bar{G}(x_i;\Omega)}{1-(1-\delta)G(x_i;\Omega)}\right]^{2\delta}\right)^{b}\right]\right)\right\}.\end{aligned}$$

The MLEs of the parameters b, δ, θ and Ω_k can be obtained by solving the nonlinear equation $\left(\frac{\partial\ell}{\partial b}, \frac{\partial\ell}{\partial\delta}, \frac{\partial\ell}{\partial\theta}, \frac{\partial\ell}{\partial\Omega_k}\right)^T = \mathbf{0}$ using iterative methods in R. See **web appendix** for individual components of the score vector.

4.2. Estimation in the Presence of Censoring

Survival time studies often involve censored observations, which means that only partial information is available during the period under study. Interval censoring can occur when an observation requires follow-up or inspections. Right censoring is a type of interval censoring that is commonly used in medical studies. This type of censoring occurs when the study ends before all units fail. Suppose we have a study with a random sample of n patients, each with an independent censoring time $Y_k; k = 1, 2, 3, ...n$, which is time interval between entry and study completion, and the failure time $X_k; i = 1, 2, ..., n$ of the i^{th} patient. It is assumed that X_k and Y_k are independent and follow the TL-HT-GPS CoDs. For $T_k = min(X_k, Y_k), (T_k, \zeta_k)$ is observed for $\zeta_k = 1$ if failure has occurred and $\zeta_k = 0$ if censoring has occurred. Consequently, the log-likelihood function (ℓ) can be expressed as

$$\ell = \sum_{k=1}^{n}\zeta_k\log\left(f(t_k)\right) + \sum_{k=1}^{n}\left(1-\zeta_k\right)\log\left(S(t_k)\right), \tag{18}$$

where $f(.)$ is the pdf of TL-HT-GPS CoDs and $S(.) = 1 - F(.)$ represent the survival function, respectively. The log-likelihood function presented in Equation (18) can be optimized using numerical methods to obtain the maximum likelihood estimates (MLEs) of the model parameters.

5. Risk Measures

Risk measures, such as value at risk (VaR), tail value at risk (TVaR), tail variance (TV), and tail variance premium (TVP), serve as statistical tools utilized by actuaries to assess market risk. Their evolution in statistics and finance is vital for effectively managing uncertainty, gaining insights into potential risks, and informing strategic decisions to mitigate adverse outcomes. Within insurance, these measures assist in risk pricing and upholding financial stability, while in finance, they are essential for portfolio evaluation and enhancing resilience by optimizing risk-return trade-offs. Integration of these risk measures into risk management frameworks empowers organizations to navigate uncertainties and make well-informed decisions.

5.1. VaR

VaR is a statistical measure that quantifies the potential magnitude of financial losses that a firm, portfolio, or specific position may face within a defined time period. It serves as a valuable metric for assessing and understanding the extent of potential downside risks in the financial realm. VaR_q, which is the q^{th} quantile for

the TIHT-GPS CoDs is calculated from

$$X_q = G^{-1}\left[\frac{\left(1-\left[\frac{\theta-[C^{-1}C(\theta)(1-q)]}{\theta}\right]^{\frac{1}{b}}\right)^{\frac{1}{2\delta}}}{1+(1-\delta)\left(1-\left[\frac{\theta-[C^{-1}C(\theta)(1-q)]}{\theta}\right]^{\frac{1}{b}}\right)^{\frac{1}{2\delta}}}\right], \tag{19}$$

where $q \in (0,1)$ is the probability threshold.

5.2. TVaR

TVaR is a quantitative measure that assesses the expected loss magnitude when an event surpasses a predetermined probability level. The TVaR for the TL-HT-GPS CoDs is

$$\begin{aligned} TVaR_q &= E\left(X|X>x_q\right) = \frac{1}{1-q}\int_{VaR_q} xf(x)dx \\ &= \frac{1}{1-q}\sum_{j=0}^{\infty}\int_{VaR_q}^{\infty} x\eta_{r+1}g_{r+1}(x;\Omega)dx, \end{aligned} \tag{20}$$

where $g_{r+1}(x;\Omega) = (r+1)G^r(x;\Omega)g(x;\Omega)$ is the exponentiated-G (Expo-G) pdf with power parameter $(r+1)$ and η_{r+1} is as given in Equation (17).

5.3. TV

TV is a statistical measure that evaluates the conditional variance of losses exceeding the VaR at a specified probability level, providing valuable insights into the risk dynamics associated with extreme outcomes. The TV_q of the TL-HT-GPS CoDs is given by

$$\begin{aligned} TV_q &= E\left(X^2 \mid X>x_q\right) - \left(TVaR_q\right)^2 = \frac{1}{1-q}\int_{VaR_q}^{\infty} x^2 f(x)dx - \left(TVaR_q\right)^2 \\ &= \frac{1}{1-q}\sum_{r=0}^{\infty}\upsilon_{r+1}\int_{VaR_q}^{\infty} x^2 g_{r+1}(x;\Omega)dx - \left(TVaR_q\right)^2, \end{aligned} \tag{21}$$

where $g_{r+1}(x;\Omega) = (r+1)G^r(x;\Omega)g(x;\Omega)$ is the Expo-G distribution with power parameter $(r+1)$, parameter vector Ω and η_{r+1} is as given in Equation (17). Hence, the TV_q of TL-HT-GPS CoDs can be obtained from those of Expo-G distributions.

5.4. TVP

Risk managers become concerned when risks exceed specific levels. Such circumstances are widespread in insurance, such as deductible plans and reinsurance contracts. Tail value premium answers demands to these circumstances. The TVP of the TL-HT-GPS CoD is expressed as

$$TVP_q = TVaR_q + \beta(TV_q), \tag{22}$$

where $0<\beta<1$. The TVP of the TL-HT-GPS CoD is found by inserting Equations (20) and (21) into Equation (22).

5.5. Numerical Study for the Risk Measures

We present results from the numerical simulations for the risk measures of the TL-HT-LLOGP distribution in this subsection. The risk metrics (TVaR, VaR, TV and TVP) of the TL-HT-LLOGP distribution are compared to the type

I heavy-tailed Weibull (TIHT-W) distribution by Zhao et al. [24], the heavy-tail log-logistic Poisson (HT-LLOGP), the log-logistic Weibull-Poisson (LLOGWP) distribution by Oluyede et al. [21], the heavy-tail log-logistic (HT-LLOG), the log-logistic Poisson (LLOGP) and the Weibull distributions. Simulation results are obtained based on the following:

(1) a series of random samples, each consisting of 100 data points, are generated for each of the distributions under consideration. The parameters associated with these distributions are estimated using the maximum likelihood technique.
(2) the calculations for the risk metrics of these distributions are performed through 1000 repetitions to ensure accurate and reliable estimates.

Table 1. Findings Derived from the Numerical Simulation of the Risk Measures

		Significance Level					
Distribution	Risk measure	0.75	0.8	0.85	0.9	0.95	0.99
TL-HT-LLOGP($b = 1.3, \theta = 0.6, \delta = 1.4, \beta = 1.7$)	VaR	36.4513	38.7442	48.5754	53.3817	76.5251	94.6520
	TVaR	52.1343	56.2249	69.8559	71.4539	82.5611	101.7086
	TV	201.4752	267.7756	293.1283	302.8258	951.8390	1398.641
	TVP	309.2408	314.8454	329.9150	341.0971	1854.248	3166.6550
TIHT-W($\alpha = 1.3, \theta = 0.6, \gamma = 1.4$)	VaR	33.4243	37.5023	42.5850	49.4916	60.7943	85.4688
	TVaR	49.3077	53.1095	57.9260	64.5664	75.5611	99.7086
	TV	214.0337	257.4698	280.9098	294.4029	303.2769	309.5669
	TVP	281.4828	295.7310	308.1684	317.3852	320.1575	311.6020
HT-LLOGP($\theta = 0.6, \delta = 1.4, \beta = 1.7$)	VaR	29.0828	31.4845	32.5431	36.18364	51.0012	65.3564
	TVaR	38.2216	44.0015	52.0692	57.0424	61.2341	79.2430
	TV	88.3543	101.3245	131.4256	162.0423	173.2123	191.2340
	TVP	201.3425	232.2402	245.4232	252.2234	355.2774	374.2108
LLOGWP($c = 1.2, a = 0.86, \beta = 1.7, \theta = 0.6$)	VaR	0.2205	0.7520	1.0017	1.4613	1.0461	1.7105
	TVaR	2.0798	2.4351	2.7523	3.0017	3.9087	4.4658
	TV	5.0713	6.7754	7.4513	7.2210	8.0912	10.1237
	TVP	12.1353	13.0087	14.1046	14.8401	16.1432	20.1244
HT-LLOG($\delta = 1.4, \beta = 1.7$)	VaR	9.3322	11.8758	14.0543	16.0987	18.4096	21.0864
	TVaR	18.2098	20.0860	21.3320	23.907	30.4223	32.0986
	TV	29.9008	31.4861	39.3265	42.597	45.0071	49.6506
	TVP	53.0978	55.0985	59.0871	60.0876	62.1290	71.0863
LLOGP($\theta = 0.6, \beta = 1.7$)	VaR	3.2944	4.0921	6.0293	7.0844	9.0432	11.0012
	TVaR	12.9944	13.0012	15.5990	17.0122	19.0932	21.0382
	TV	23.2103	24.9577	25.7855	26.3943	29.1355	30.0533
	TVP	33.2058	34.4832	36.1103	27.0543	42.1039	44.9584
Weibull($\alpha = 1.3$)	VaR	1.4296	1.6908	2.0349	2.5321	3.4106	5.5595
	TVaR	2.2893	2.4380	2.5990	2.7727	2.9589	3.1618
	TV	1.2220	1.4581	1.8565	2.5417	3.7671	4.8106
	TVP	3.2058	3.6045	4.1771	5.0603	6.5376	7.9243

Table [1] presents the numerical risk measure results for the heavy-tailed distributions. The TL-HT-LLOGP distribution is recommended for modeling heavy-tailed data due to its elevated risk measure values in comparison to the LLOGWP, TIHT-W and the Weibull distributions.

6. Simulations

Simulation results hold significant implications for practical applications by offering insights into system behavior and performance, guiding decision-making processes, optimizing strategies, assessing risks, and testing hypotheses in controlled environments. Analyzing these results enables informed choices, prediction of outcomes, identification of challenges, and refinement of strategies to enhance efficiency, mitigate risks, and drive innovation across diverse domains such as manufacturing, healthcare, finance, and engineering.

In order to evaluate the consistency of MLEs, a simulation study was performed. The results providing an overview of the findings are displayed in Table [2]. We simulated for n= 25, 50, 100, 200, 400 and 800 and for N=3000 from the TL-HT-LLOGP distribution. The average bias (AvBIAS) and root mean square error (RMSEr) for an estimated parameter, say ($\hat{\delta}$), is calculated using the formulae

$$AvBIAS(\hat{\delta}) = \frac{\sum_{i=1}^{N} \hat{\delta}_i}{N} - \delta, \quad \text{and} \quad RMSEr(\hat{\delta}) = \sqrt{\frac{\sum_{i=1}^{N} (\hat{\delta}_i - \delta)^2}{N}},$$

respectively. Analyzing the outcomes presented in Table [2], we note that the average values closely approximate the true parameter values. Furthermore, the RTMSEr and AvBIAS tend to diminish towards zero for all parameters with increasing sample size, indicating improved accuracy and reduced estimation errors. This shows that the TL-HT-LLOGP distribution produces efficient parameters estimates.

Table 2. Monte Carlo Simulation Results for TL-HT-LLOGP: Mean, RMSEr, and AvBias

		$b=0.5,\theta=2.5,\delta=2.5,\beta=1.5$			$b=1.2,\theta=0.2,\delta=0.1,\beta=1.2$		
	n	Mean	RMSEr	AvBIAS	Mean	RMSEr	AvBIAS
b	25	0.9296	1.8639	0.4796	1.7813	0.8995	0.5813
	50	0.8992	1.6721	0.3992	1.5371	0.5853	0.3371
	100	0.6242	0.3772	0.1242	1.3859	0.3515	0.1859
	200	0.5663	0.2329	0.0663	1.3566	0.2625	0.1566
	400	0.5616	0.2270	0.0616	1.2836	0.1413	0.0836
	800	0.5517	0.1601	0.0517	1.2479	0.0998	0.0379
θ	25	3.0294	1.8093	0.5294	1.4079	1.6445	1.2079
	50	2.9007	1.5547	0.4007	1.1755	1.3241	0.9755
	100	2.7672	1.4978	0.2672	1.0402	1.2778	0.8402
	200	2.5553	0.9077	0.2553	0.7288	0.7759	0.5288
	400	2.5473	0.8849	0.2073	0.4323	0.5157	0.2823
	800	2.5078	0.5218	0.1678	0.2497	0.2082	0.1007
δ	25	4.6348	5.1003	2.1348	0.0701	0.0645	-0.0199
	50	3.5526	3.1127	1.0526	0.0750	0.0586	-0.0050
	100	2.9448	1.6884	0.4448	0.0809	0.0445	-0.0050
	200	2.6216	0.9167	0.1216	0.0901	0.0333	-0.0039
	400	2.5073	0.6202	0.0073	0.0987	0.0234	-0.0023
	800	2.4601	0.3116	-0.0399	0.1012	0.0180	0.0020
β	25	1.9431	1.2952	0.4431	2.2217	1.9376	1.0217
	50	1.7955	1.0873	0.2955	1.8060	1.3262	0.4060
	100	1.6885	0.8178	0.1885	1.7115	0.2256	0.0915
	200	1.6203	0.6372	0.1203	1.5839	0.1961	0.0861
	400	1.6049	0.6061	0.1149	1.3350	0.1711	0.0450
	800	1.5108	0.4296	0.0108	1.2001	0.1404	0.0092

		$b=0.5,\theta=1.5,\delta=3.0,\beta=3.0$			$b=0.5,\theta=3.0,\delta=3.0,\beta=3.0$		
	n	Mean	RMSEr	AvBIAS	Mean	RMSEr	AvBIAS
b	25	1.1222	2.1448	0.9222	0.9050	2.4723	0.7050
	50	0.9271	1.2679	0.7271	0.7773	1.9103	0.5773
	100	0.6304	0.7296	0.5304	0.5764	0.3364	0.0764
	200	0.5719	0.4998	0.3281	0.5537	0.2306	0.0537
	400	0.5331	0.2512	0.1469	0.5279	0.2176	0.0279
	800	0.5010	0.1155	0.0390	0.5134	0.1313	0.0134
θ	25	2.8695	2.5363	0.8695	3.2879	2.0257	0.2879
	50	2.0452	1.4912	0.8352	3.1839	1.4032	0.0739
	100	1.8265	1.4635	0.8265	3.1109	1.3524	0.0639
	200	1.6437	1.3887	0.7437	3.0789	1.2206	0.0289
	400	1.5916	1.3056	0.6516	3.0089	0.6757	0.0089
	800	1.5182	1.1831	0.4582	3.0003	0.4109	0.0023
δ	25	4.4494	1.8709	2.4494	5.2262	4.9147	3.2262
	50	3.8855	1.2993	1.2855	4.2056	3.3279	1.7056
	100	3.4636	0.8682	0.4636	3.7425	2.2571	0.7425
	200	3.2656	0.6134	0.2656	3.2597	1.2883	0.2597
	400	3.1490	0.3233	0.1490	3.1019	0.8085	0.0609
	800	3.0492	0.1270	0.0492	3.0342	0.5863	0.0042
β	25	4.0077	1.5524	1.0077	3.7774	2.3588	0.7774
	50	3.9403	1.3931	0.9403	3.4693	1.8713	0.4693
	100	3.8333	1.1406	0.8333	3.3877	1.4518	0.3877
	200	3.7647	0.9214	0.7647	3.1716	1.0639	0.1716
	400	3.4830	0.7417	0.4270	3.1568	0.8919	0.1568
	800	3.2196	0.4133	0.2186	3.0977	0.6919	0.0977

7. Applications

Applying probability distributions to datasets poses challenges like assumption violations, outlier influence, and multimodal distribution complexities. Overcoming these hurdles demands a profound dataset understanding, exploration of diverse distributional forms, and the employment of robust statistical methods for accurate modeling outcomes.

The objective of this section is to showcase the adaptability and applicability of the TL-HT-GPS CoDs, highlighting their versatility and usefulness in practical contexts. We focus on one of its special cases, the TL-HT-LLOGP distribution, and apply it to two real data sets. The GoF statistics used included: $-2\log(L)$, Akaike Information Criterion (AIC), Consistent Akaike Information Criterion (CAIC), Bayesian Information Criterion (BIC), Cramér-von Mises (CVM), Anderson-Darling (AD), and the Kolmogorov-Smirnov (K-S) statistics and its associated p-value. We gave preference to the model with the highest K-S statistics p-value and lower GoF statistics. To estimate the TL-HT-LLOGP model parameters, we used the non-linear minimization (**nlm**) function from the R software, and the parameter estimates were presented together with their standard errors (in parenthesis).

We compared the TL-HT-LLOGP model with several non-nested models, along with some well-known heavy-tailed models. The competing distributions are as follows: Topp-Leone Weibull Lomax (TLWLx) by Jamal et al. [10], type I heavy-tailed Weibull (TIHT-W) by Zhao et al. [24], heavy-tailed beta power transformed Weibull (HTBPTW) by Zhao et al. [23], exponentiated Half logistic log-logistic Poisson (EHLLLOGP) by Chipepa et al. [7], log-logistic Weibull-Poisson (LLOGWP) by Oluyede et al. [21], exponential Lindley odd log-logistic Weibull (ELOLLW) by Korkmaz et al. [12], and odd exponentiated half logistic Burr XII (OEHLBXII) by Aldahlan and Afify [1]. The pdfs of the competing distributions are presented in the **web appendix**. Profile plots were presented on all data sets to verify the uniqueness of the parameter estimates.

We also presented the sum of squares (SS) obtained from the probability plots to calculate closeness to the diagonal line. SS is given as

$$SS = \sum_{j=1}^{n} \left[F_{TL-HT-LLOGP}(x_{(j)}; \hat{b}, \hat{\theta}, \hat{\delta}, \hat{\beta}) - \left(\frac{j - 0.375}{n + 0.25} \right) \right]^2, j = 1, 2, ..., n,$$

where $x_{(j)}$ is the j^{th} ordered observed data value. In addition to the probability plots, the fitted densities, empirical cumulative distribution function (ECDF), Kaplan-Meier (K-M) survival curve, total time on test (TTT) plots, and hazard rate function (hrf) plots were also presented.

7.1. Growth Hormone Data

Human growth hormone, or somatotropin, is a single-chain polypeptide composed of amino acids produced by somatotropic cells in the anterior pituitary gland (Brinkman et al. [5]). Initially recognized for its role in regulating growth during childhood, human growth hormone is a vital hormone with diverse physiological functions. The initial data set provides the estimated duration between the administration of growth hormone medication to the attainment of the target age in the *Programa Hormonal de Secretaria de Saude de Minas Gerais* in 2009, according to Alizadeh et al. [2]. The data is presented in the **web appendix**.

Table 3. Estimates and GoF Statistics for Growth Hormone Data

Distribution	Estimates and SEs				GoF Statistics							
					-2log(L)	AIC	CAIC	BIC	CVM	AD	K-S	p−value
	b	θ	δ	β								
TL-HT-LLOGP	2.3713	75.1001	9.24×10^{-3}	8.4912	154.2595	162.2595	163.5928	168.4809	0.0318	0.2201	0.0731	0.9920
	(0.9661)	(0.0405)	(3.58×10^{-3})	(3.6358)								
	a	b	α	θ								
TLWLx	0.1797	137.5700	1.4816	378.2200	155.1652	163.1652	164.4985	169.3866	0.0344	0.2471	0.0859	0.9585
	(0.0124)	(4.78×10^{-4})	(0.2281)	(2.11×10^{-4})								
	α	θ	γ									
TIHT-W	1.7227	0.0530	1.0247	-	158.1126	164.1126	164.8868	168.7787	0.0818	0.5380	0.1324	0.5716
	(0.2462)	(0.0383)	(0.4408)									
	α	γ	β									
HTBPTW	1.9932	0.0279	1.2113	-	164.9772	170.9722	171.7514	175.6432	0.1639	1.0262	0.1454	0.4500
	(0.2437)	(0.0147)	(0.8232)									
	δ	β	λ	θ								
EHLLLOGP	11.1020	0.2133	11.1030	2.46×10^{-8}	155.4615	163.4615	164.7948	169.6829	0.0426	0.2836	0.0965	0.9003
	(0.0657)	(0.0274)	(20.8230)	(0.0153)								
	c	α	β	θ								
LLOGWP	2.5303	2.13×10^{-5}	1.21×10^{-3}	29.1180	155.5916	163.5963	164.9250	169.8130	0.0414	0.2812	0.0920	0.9287
	(0.3044)	(0.3222)	(2.4859)	(14.2210)								
	β	λ	θ	γ								
ELOLLW	112.6600	0.7844	0.2513	1.4016	162.0931	170.0931	171.4265	176.3145	0.1257	0.8010	0.1331	0.5648
	(4.07×10^{-4})	(1.1037)	(0.4958)	(0.1667)								
	α	λ	a	b								
OEHLBXII	0.4337	4.15×10^{-3}	19.5340	0.1386	183.2823	191.2823	192.6157	197.5037	0.2656	1.6324	0.1966	0.1338
	(0.1799)	(9.19×10^{-3})	(3.08×10^{-4})	(0.0434)								

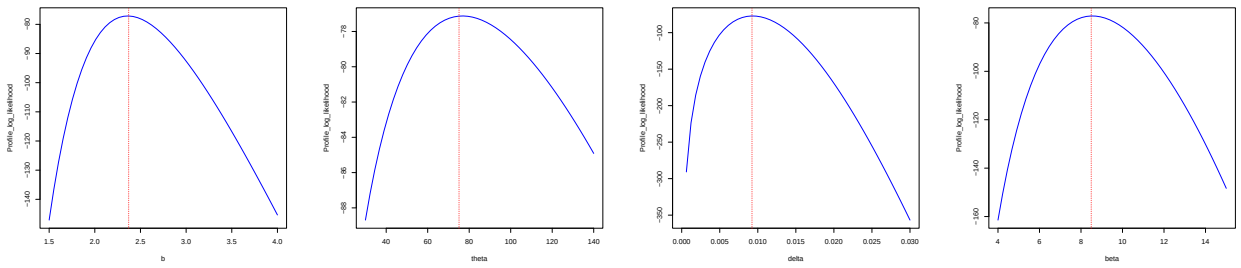

(a) (b) (c) (d)

Figure 7. Profile plots of the TL-HT-LLOGP on growth hormone data

From Table [3], we can draw the conclusion that the TL-HT-LLOGP distribution is superior to the contending non-nested models. The p-values clearly show how the TL-HT-LLOGP model out-performs the other models. The profile plots in Figure [7] show that the TL-HT-LLOGP distribution parameters on growth hormone data may be uniquely identified.

The asymptotic confidence intervals at 95% confidence level for the model parameters are as follows: $b \in [2.3713 \pm 1.8936]$, $\theta \in [75.1001 \pm 0.0794]$, $\delta \in [9.24 \times 10^{-3} \pm 7.02 \times 10^{-3}]$ and $\beta \in [8.4912 \pm 7.1262]$.

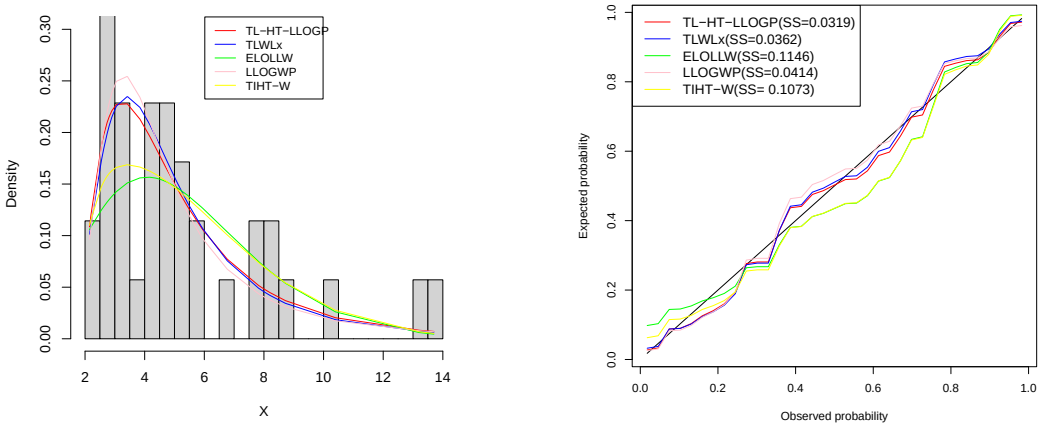

(a) (b)

Figure 8. Fitted densities and probability plots for growth hormone data

Figure [8] depicts the density functions superimposed on a histogram of growth hormone data as well as plots of the observed probability versus their expected probabilities for the TL-HT-LLOGP distribution and the contending distributions. In comparison, the TL-HT-LLOGP distribution fits better as evidenced by the smallest SS value provided in the probability plots.

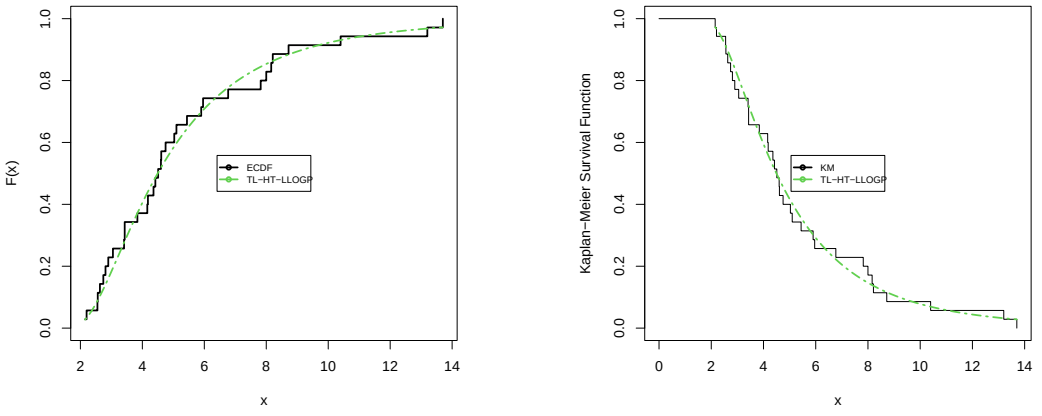

(a) (b)

Figure 9. Fitted ECDF curve and K-M survival plots for growth hormone data

Figure [9] presents the comparison between the observed and fitted ECDF and K-M survival curves for the growth hormone data. The graphs show that the TL-HT-LLOGP distribution closely aligns with the ECDF and K-M survival curves.

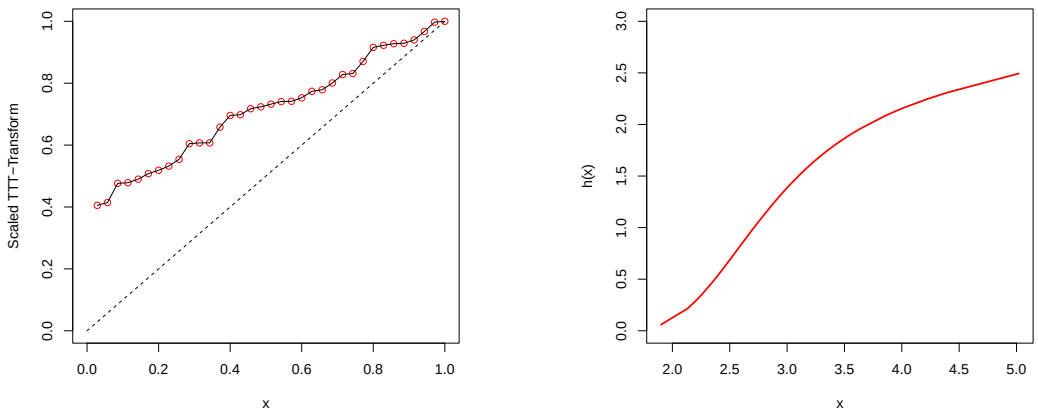

(a) (b)

Figure 10. Fitted TTT scaled and hrf plots for growth hormone data

Observing the TTT scaled plot and hrf plot depicted in Figure [10], it can be inferred that the data exhibits an increasing hazard rate pattern.

7.2. Data on Head and Neck Cancer

This data set encompasses the observed duration of survival for a cohort comprising forty-nine (49) individuals who have received a diagnosis of head and neck cancer. Efron [8] and Lee et al. [13]) conducted the analysis of the data, which can be found in the supplementary materials in the **web appendix**.

7.2.1. Head and Neck Cancer Data (Complete Case): This subsection contains parameter estimates, standard errors (SEs) of the estimates (in parentheses), GoF statistics, fitted densities, probability plots, K-M survival plot, ECDF plot, TTT plot and hrf plot for forty (40) complete observations.

Table 4. Estimates of Parameters and GoF Statistics for the Head and Neck Cancer Data

					GoF Statistics							
Distribution	**Estimates and SEs**				**-2log(L)**	**AIC**	**CAIC**	**BIC**	**CVM**	**AD**	**K-S**	**p−value**
	b	θ	δ	β								
TL-HT-LLOGP	79.7650	30.3610	1.1168	0.1865	526.1938	534.1938	535.3366	540.9493	0.1184	0.6575	0.1216	0.5955
	(2.59×10^{-4})	(1.11×10^{-4})	(0.0566)	(0.0262)								
	a	b	α	θ								
TLWLx	0.0555	110.8200	5.6544	3.4617	526.2917	534.2917	535.4446	541.0572	0.1216	0.6737	0.1258	0.5512
	(2.96×10^{-3})	(4.07×10^{-4})	(2.0769)	(2.8330)								
	α	θ	γ									
TIHT-W	1.2407	2.9439	1.22×10^{-4}	-	529.1013	535.1013	535.7686	541.0339	0.1976	1.0838	0.1790	0.3542
	(0.1434)	(2.62×10^{-4})	(1.05×10^{-4})									
	α	γ	β									
HTBPTW	1.0731	2.28×10^{-3}	0.9898	-	530.5814	536.5814	537.2481	541.6480	0.2232	1.2357	0.1564	0.2822
	(0.1225)	(1.75×10^{-3})	(0.8787)									
	δ	β	λ	θ								
EHLLLOGP	224.2000	3.7208	0.3020	1.14×10^{-4}	538.1685	546.1685	547.3114	552.9240	0.2131	1.2998	0.1643	0.2305
	(9.18×10^{-7})	(3.43×10^{-3})	(3.85×10^{-5})	(0.0408)								
	c	α	β	θ								
LLOGWP	0.4413	1.6264	0.1844	309.2200	530.3653	538.3653	539.5081	545.1208	0.1372	0.8189	0.1302	0.5067
	(0.4393)	(0.5041)	(0.0489)	(1.53×10^{-3})								
	β	λ	θ	γ								
ELOLLW	433.1800	0.5301	0.0505	0.7517	527.9126	535.9126	537.0555	542.6681	0.1750	0.9604	0.1490	0.3371
	(6.80×10^{-5})	3.4885)	(0.2499)	(0.0847)								
	α	λ	a	b								
OEHLBXII	0.3914	5.18×10^{-5}	3.3566	0.4750	552.6883	560.6883	561.8311	567.4438	0.3962	2.2403	0.2191	0.0429
	(0.0308)	(4.33×10^{-5})	(5.23×10^{-3})	(0.0370)								

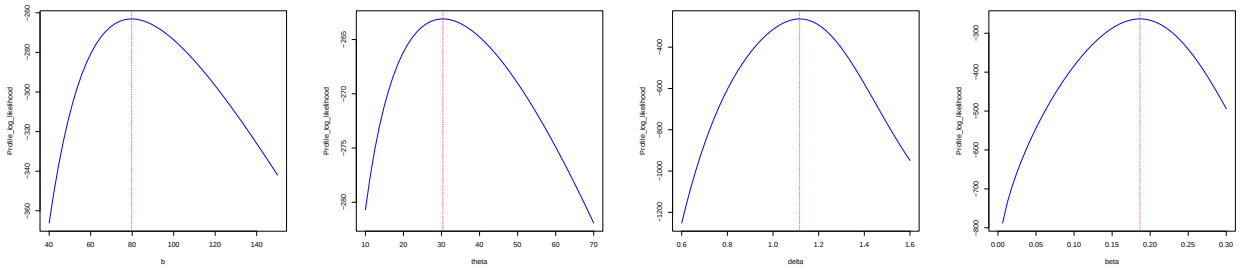

(a) (b) (c) (d)

Figure 11. Profile plots of the TL-HT-LLOGP: Head and neck cancer data

From Table [4], we can draw the conclusion that the TL-HT-LLOGP model is superior to the contending non-nested models. The profile plots in [11] give evidence that the TL-HT-LLOGP parameters on head and neck cancer data can be uniquely determined.

The model parameters are estimated with 95% asymptotic confidence intervals as follows: $b \in [79.7650 \pm 5.08 \times 10^{-4}]$, $\theta \in [30.3610 \pm 2.18 \times 10^{-4}]$, $\delta \in [1.1168 \pm 0.1109]$ and $\beta \in [0.1865 \pm 0.0514]$.

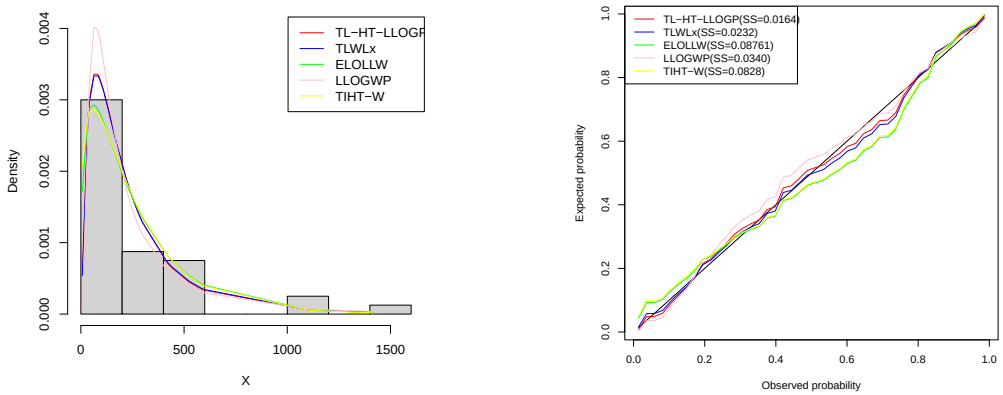

Figure 12. Density and probability plots for head and neck cancer

Figure [12] depicts the density functions superimposed on a histogram of head and neck cancer data, as well as plots of the observed probability versus the expected probabilities of the TLHTLLOGP distribution and various competing distributions. In comparison, the TL-HT-LLOGP distribution fits better.

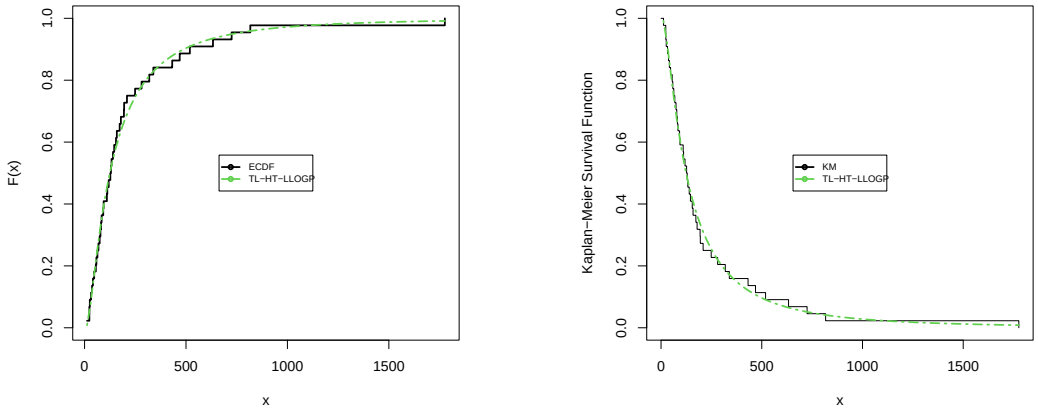

(a) (b)

Figure 13. Plots of the fitted ECDF curve and K-M survival plots for the head and neck cancer data

Figure [13] displays the fitted ECDF and K-M survival curves both based observed for head and neck cancer data. The graphs show that the TL-HT-LLOGP distribution closely follow the ECDF and K-M survival curves.

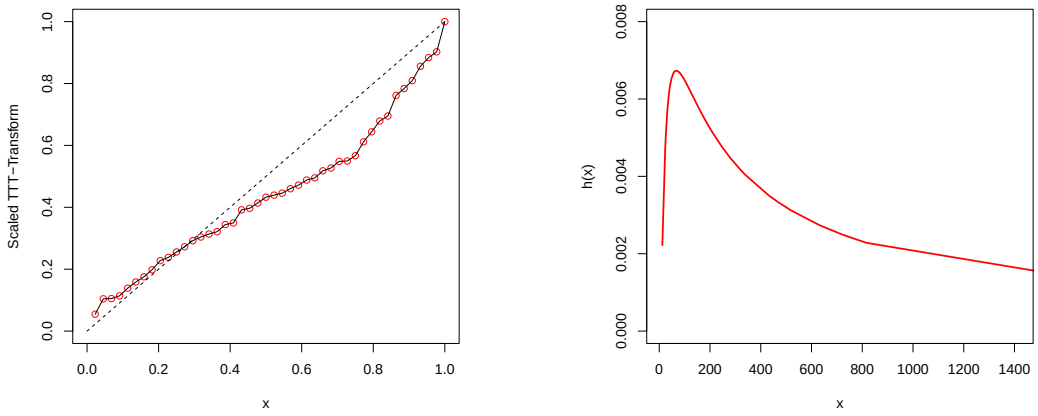

(a) (b)

Figure 14. Fitted TTT caled and hrf plots for head and neck cancer data

The complementary analysis of the TTT scaled and hrf plots in Figure [14] suggest that, the data follow an upside-down bathtub hazard rate shape.

7.2.2. Head and Neck Cancer Data (Censored Case): This section contains parameter estimates and GoF statistics for head and neck cancer data including censored observations. The data is contained in the **web appendix**.

Table 5. Parameter Estimates and GoF Statistics: Censored Case

Distribution	Estimates and SEs				GoF Statistics				
					-2log(L)	AIC	CAIC	BIC	SS
TL-HT-LLOGP	b	θ	δ	β	559.3177	567.3177	568.2268	574.8850	0.0361
	3.3755	42.7234	0.0737	0.8863					
	(0.9687)	(0.0270)	(0.0496)	(0.3501)					
TLWLx	a	b	α	θ	559.5581	567.5581	568.4672	575.1254	0.0423
	0.0563	1.90×10^{3}	3.2538	9.2257					
	(8.41×10^{-4})	(5.21×10^{-5})	(0.3823)	(0.0519)					
TIHT-W	α	θ	γ		564.5581	570.5581	571.0914	576.2336	0.0593
	1.0230	2.6973	3.28×10^{-4}	-					
	(0.1236)	(4.23×10^{-4})	(2.52×10^{-5})						
HTBPTW	α	γ	β		566.8449	572.8449	568.3782	578.5244	0.0604
	0.9141	3.89×10^{-3}	0.9999	-					
	(0.1106)	(2.77×10^{-3})	(0.7409)						
EHLLLOGP	δ	β	λ	θ	562.1811	570.1811	571.0902	577.7484	0.0561
	14.5281	0.0248	20.9891	3.5890					
	(3.9227)	(8.52×10^{-3})	(4.2365)	(1.6813)					
LLOGWP	c	α	β	θ	586.0382	594.0382	594.9473	601.6055	0.0732
	0.0589	7.64×10^{-3}	0.8612	3.6817					
	(0.2526)	(0.0177)	(0.2961)	(1.3379)					
ELOLLW	β	λ	θ	γ	563.7936	571.7936	572.7027	579.3609	0.0589
	236.4900	7.0294	0.0149	0.6234					
	(1.28×10^{-8})	(5.48×10^{-6})	(8.85×10^{-3})	(0.0733)					
OEHLBXII	α	λ	a	b	587.8382	595.8382	596.7473	603.4055	0.0711
	0.5647	1.20×10^{-3}	1.2497	0.8457					
	(0.1172)	(9.86×10^{-3})	(0.2374)	(0.1621)					

Table [5] gives the MLEs with their corresponding SEs (in parentheses) of the unknown parameters of the TL-HT-LLOGP distribution for the censored data found by maximizing the log-likelihood function in Equation (18). The asymptotic confidence intervals at a 95% confidence level for the model parameters are: $b \in [3.3755 \pm 1.8987]$, $\theta \in [42,7234 \pm 0.0530]$, $\delta \in [0.0737 \pm 0.0972]$ and $\beta \in [0.8863 \pm 0.0682]$, respectively.

The analysis of the GoF statistics shown in Tables [5] provides compelling evidence that the TL-HT-LLOGP model exhibits superior performance than its selected non-nested models when applied to the censored head and neck cancer data.

8. Summary

In summary, the current study has made significant contributions to the field of statistical modeling by introducing the TL-HT-GPS CoDs. This novel class of continuous distributions has demonstrated the ability to effectively model heavy-tailed data and a wide range of hazard rate patterns, both monotonic and non-monotonic. The comprehensive investigation of the statistical properties of the TL-HT-GPS CoDs, along with the successful implementation of the MLE technique for parameter estimation, has strengthened the theoretical and practical applicability of this distribution. The study's comparative analysis has demonstrated the superior performance of the TL-HT-LLOGP CoDs, a member of the TL-HT-GPS CoDs, in fitting real-life data sets when compared to existing non-nested models. This highlights the flexibility and adaptability of the TL-HT-GPS distribution in handling a wide range of data, including cases with censored observations.

While the current study has laid a solid foundation for the TL-HT-GPS CoDs, there remain several avenues for future research. Exploring other members of the TL-HT-GPS CoDs and their potential applications, investigating the performance of the distribution in modeling specific types of real-life data and other statistical properties could lead to valuable insights. The application of TL-HT-GPS CoDs in areas such as risk management, survival analysis, and reliability engineering holds significant promise. Additionally, extending this distribution to the multivariate case through copula-based extensions and exploring Bayesian estimation techniques offer compelling avenues for future research. Overall, the present study has paved the way for further advancements in the realm of statistical modeling and data analysis.

Appendix

To access the appendix, kindly click on the link provided below:
https://drive.google.com/file/d/1xXdo1rCGBsiixLthkSd8fJUVDmdpKqAP/view?usp=sharing

REFERENCES

1. Aldahlan, M., and Afify, A. Z, *The odd exponentiated half-logistic Burr XII distribution*, Pakistan Journal of Statistics and Operation Research, vol. 14, no. 2, pp. 305-317, 2018.
2. Alizadeh, M., Bagheri, S., Bahrami, S. E., Ghobadi, S., and Nadarajah, S, *Exponentiated Power Lindley Power Series Class of Distributions: Theory and Applications*, Communications in Statistics-Simulation and Computation, vol. 47, no. 9, pp. 2499–2531, 2018.
3. Al-Shomrani, A., Arif, O., Shawky, A., Hanif, S., and Shahbaz, M. Q, *Topp-Leone family of distributions: Some properties and applications*, Pakistan Journal of Statistics and Operation Research, vol. 12, no. 3, pp. 443–451, 2016.
4. Al-Zahrani, B, *Goodness-of-fit for the Topp-Leone distribution with unknown parameters*, Applied Mathematical Sciences, vol. 6, no. 128, pp. 67–98, 2012.
5. Brinkman, J.E., Tariq, M.A., Leavitt, L., and Sharma, S, *Physiology, growth hormone*, StatPearls, 2020.
6. Chesneau, C., Sharma, V. K., and Bakouch, H.S, *Extended Topp-Leone family of distributions as an alternative to beta and Kumaraswamy type distributions: Application to glycosaminoglycans concentration level in urine*, International Journal of Biomathematics, vol. 14, no. 2, pp. 205-238, 2021.
7. Chipepa, F., Oluyede, B., Chamunorwa S., Makubate, B., and Zidana, C, *The exponentiated half logistic-generalized-G Power series class of distributions: Properties and applications*, Journal of Probability and Statistical Science, vol. 20 no. 1, pp. 21-40, 2022.
8. Efron, B, *Logistic regression, survival analysis, and the Kaplan-Meier curve*, Journal of the American Statistical Association, vol. 83 no. 402, pp. 414–425, 1988.
9. Ghitany, M. E., Kotz, S., and Xie, M, *On some reliability measures and their stochastic orderings for the Topp-Leone distribution*, Journal of Applied Statistics, vol. 32, no. 7, pp. 705-722, 2005.
10. Jamal, F., Reyad, H. M., Nasir, M. A., Chesneau, C., Shah, M. A. A., and Ahmed, S. O, *Topp Leone Weibull-Lomax distribution: Properties, regression model and applications*, NED University Journal of Research, vol. 17, no. 4.
11. Johnson, N. L., Kotz, S., and Balakrishnan, N, *Continuous distributions, John Wiley and Sons, New York*, Statistics Applications and Probability, vol. 1, pp. 105-122, 1994.
12. Korkmaz, M. C., Yousof, H. M., and Hamedani, G. G, *The exponentiated half logistic-generalized-G Power series class of distributions: Properties and applications*, Journal of Statistical Theory and Applications, vol. 17 no. 3, pp. 554-571, 2018.
13. Lee, C., Famoye, F., and Olumolade, G. G. *Beta-Weibull distribution: Some properties and applications to censored data*, Journal of Modern Applied Statistical Methods, vol. 6 no. 1, pp. 173-186, 2007.
14. Mcdonald, J. B., and Butler, R. B, *Using incomplete moments to measure inequality*, Journal of Econometrics, vol. 42 no. 1, pp. 109–119, 1989.
15. Moakofi, T., Oluyede, B., and Chipepa, F, *Type II exponentiated half-logistic-Topp-Leone-G power series class of distributions with applications*, Pakistan Journal of Statistics and Operations Research, vol. 17 no. 4, pp. 885–909, 2021.
16. Moakofi, T., Oluyede, B., and Gabanakgosi, M, *The Topp-Leone Odd-Burr III-G family of distributions: Model, propeeties and applications*, Statistics Optimization and Information Computing, vol. 10, pp. 236–262, 2022.
17. Nadarajah, S., and Kotz, S, *Moments of some J-shaped distributions*, Journal of Applied Statistics, vol. 30 no. 3, pp. 311-317, 2003.
18. Oluyede, B., Chipepa, F., and Wanduku, D, *The Odd Weibull-Topp-Leone-G power series family of distributions: Model, properties and applications*, Journal of Nonlinear Science and Application, vol. 14 no. 6, pp. 60-65, 2021.
19. Oluyede, B., Dingalo, N., and Chipepa, F, *The Topp-Leone-Harris-G family of distributions with applications*, International Journal Mathematics in Operational Research, vol. 24 no. 4, pp. 554-582, 2023.
20. Oluyede, B., Moakofi T., and Chipepa F, *The odd power generalized Weibull-G power series class of distributions: Properties and applications*, Statistics in Transition New Series (SiTns), vol. 23 no. 1, pp. 89-108, 2022.
21. Oluyede, B., Warahena-liyanye, G., and Pararai M, *A new compound class of log-logistic Weibull-Poisson distributions: Model properties and applications*, Journal of Statistical Computation and Simulation, vol. 86, pp. 1363-1391, 2015.
22. Vicaria, D., Dorp, J. R. V., and Kotz, S, *Two-sided generalized Topp and Leone (TS-GTL) distributions*, Journal of Applied Statistics, vol. 35 no. 10, pp. 1115-1129, 2008 .
23. Zhao, W., Ahmad, Z., Mahmoudi, E., Hafez, E. H., and Mohie El-Din, M. M, *A new class of heavy-tailed distributions: Modeling and simulating actuarial measures*, Complexity, Hindawi, vol. 2021, pp. 1-18.
24. Zhao, W., Khosa, S. K., Ahmad, Z., Aslam M., and Afify, A. Z, *Type-I heavy-tailed family with applications in medicine, engineering and insurance*, PLoS ONE, vol. 15 no. 8, pp. 63-79